Design and *In Vivo* Evaluation of a Non-invasive Transabdominal Fetal Pulse Oximeter

Daniel D. Fong, Kaeli J. Yamashiro, Kourosh Vali, Laura A. Galganski, Jameson Thies, Rasta Moeinzadeh, Christopher Pivetti, André Knoesen, Vivek J. Srinivasan, Herman L. Hedriana, Diana L. Farmer, M. Austin Johnson, Soheil Ghiasi

***Abstract*— *Objective:* Current intrapartum fetal monitoring technology is unable to provide physicians with an objective metric of fetal well-being, leading to degraded patient outcomes and increased litigation costs. Fetal oxygen saturation (SpO2) is a more appropriate measure of fetal distress, but the inaccessibility of the fetus prior to birth makes this impossible to capture through current means. In this paper, we present a fully non-invasive, transabdominal fetal oximetry (TFO) system that provides *in utero* measures of fetal SpO2. *Methods:* TFO is performed by placing a reflectance-mode optode on the maternal abdomen and sending photons into the body to investigate the underlying fetal tissue. The proposed TFO system design consists of a multi-detector optode, an embedded optode control system, and custom user-interface software. To evaluate the developed TFO system, we utilized an *in utero* hypoxic fetal lamb model and performed controlled desaturation experiments while capturing gold standard arterial blood gases (SaO2). *Results:* Fetal hypoxia was induced in a graded fashion with true SaO2 values ranging between 10.5% and 66%. The non-invasive TFO system was able to accurately measure these fetal SpO2 values, supported by a root mean-squared error of 6.37% and strong measures of agreement with the gold standard. *Conclusion:* The results support the efficacy of the presented TFO system to non-invasively measure a wide-range of fetal SpO2 values and identify critical levels of fetal hypoxia. *Significance:* TFO has the potential to improve fetal outcomes by providing obstetricians with a non-invasive measure of fetal oxygen saturation prior to delivery.**

***Index Terms*— Non-invasive Medical Devices, Fetal Monitoring Technology, Pulse Oximetry, Hypoxic Fetal Lamb**

I. Introduction

OBSTETRICIANS currently evaluate fetal well-being during the intrapartum period of pregnancy (active labor) through cardiotocography (CTG), which monitors the temporal relationship of uterine contractions and fetal heart rate (FHR). The FHR tracings are displayed to an obstetrician who interprets the fetal well-being through visual inspection, where a slowly decreasing FHR may be a sign of fetal asphyxia and that surgical intervention may be needed [1]. As such, CTG was widely adopted after its introduction despite the lack of a large randomized control trial validating its efficacy, as it was deemed unethical to withhold the expected benefits from a control group [2]. However, these benefits *have not been realized*. Studies have shown that CTG does not significantly change the rates of adverse fetal outcomes associated with fetal hypoxia, including low Apgar scores, acidotic cord blood gases, and perinatal death and morbidity [3]. Rather, CTG significantly increases the rates of emergency Cesarean deliveries or C-sections, exposing both mother and child to additional risks, including higher rates of post-operative complications and chronic diseases [4], [5]. Currently, one in three children are born via C-section in the United States, where a large proportion are performed due to the presence of a non-reassuring FHR tracing (NRFT) and exceeds recommended levels from the World Health Organization [6]–[8]. Notably, NRFTs occur in 80% of all traces and its management is associated with high variability among *inter-* and *intra-* observers [9], creating a litigation nightmare and motivating the need for a more objective and accurate measure of fetal well-being. While CTG is extremely sensitive for the detection of fetal hypoxia, it has poor specificity [10]. In adults, hypoxia is detected through a pulse oximeter, commonly placed on the finger, which monitors arterial oxygen saturation (SpO2). However, the inaccessibility of the fetus prior to birth makes measuring fetal SpO2, through current means, practically impossible.

To address this problem, we have developed a transabdominal fetal pulse oximetry (TFO) system that provides a non-invasive measure of fetal SpO2 to clinicians. This technique sends photons through the maternal abdomen to investigate the deep, underlying fetal tissues. Some of the photons that reach the fetus are captured by an optical probe (optode), where the signal is processed and analyzed to extract fetal SpO2. In this work, we present a novel transabdominal fetal pulse oximeter and discuss important aspects of its design. The system was evaluated on a wide-range of fetal SpO2 through controlled desaturation experiments through an *in utero* hypoxic fetal sheep model, where invasive, gold standard measures were captured alongside the non-invasive TFO system.

Manuscript received Month dd, 2020; revised Month dd, 2020; accepted June 4, 2020. Date of publication Month dd, 2020; date of current version Month dd, 2020. This material is based upon work supported by the National Science Foundation under Grant No. IIS-1838939. Support from CITRIS and UC Davis College of Engineering are also acknowledged. *(Corresponding Author: Daniel D. Fong.)*

D. D. Fong, K. Vali, J. Thies, R. Moeinzadeh, A. Knoesen, and S. Ghiasi are with the Electrical and Computer Engineering Department, University of California Davis (e-mail: dfong@ucdavis.edu).

K. J. Yamashiro, L. A. Galganski, C. Pivetti, and D. L. Farmer are with the Department of Surgery, University of California Davis Health.

V. J. Srinivasan is with the Department of Biomedical Engineering, University of California Davis.

H. L. Hedriana is with the Department of Obstetrics and Gynecology, University of California Davis Health.

M. A. Johnson is with the Department of Surgery, University of Utah.

II. Overview of Pulse Oximetry

Pulse oximetry is a non-invasive technique that estimates relative amounts of functional hemoglobin in arterial blood by analyzing the changes in light intensity caused by pulsating arterial tissues. At a high-level, cardiac contractions cause arterial tissue to pulsate, periodically increasing the blood-tissue volume ratio, resulting in oscillations in the light intensity seen at a detector. The resulting periodic time-domain signal is called a photoplethysmogram (PPG). A PPG exhibits valleys and peaks, where each valley-to-peak excursion represents changes in arterial blood volume that correspond to systole and diastole. Since oxy- and deoxy- hemoglobin (HbO2 and Hb) absorb light at different levels for a particular wavelength, the PPG pulse depth at two wavelengths can be used to estimate the relative concentration of HbO2 in the pulsating (arterial) tissue and provide a non-invasive measure of SpO2 [11].

Analytically, this approach utilizes the differential form of the Modified Beer-Lambert Law (dMBLL) [12], [13], which relates the change in light attenuation (ΔA) to changes in the chromophore concentration between different tissue states:

$$\Delta A(\lambda) = -\ln(I_{t2}/I_{t1}) = \sum_j \Delta\mu_{a,j}(\lambda) * \langle L_j \rangle \quad (1)$$

where ΔA is the change in light attenuation and the parameters I_{t1} and I_{t2} are the measured intensities of wavelength λ at time points $t1$ and $t2$, between which the tissue composition changes. Changes in the chromophore concentrations are denoted by the change in absorption coefficients ($\Delta\mu_a$) for multiple tissues (j), and $\langle L_j \rangle$ is the expected partial path length in the j^{th} tissue. For clarity, the absorption coefficient and chromophore concentrations are related by

$$\mu_a = \ln(10) * \sum_i \epsilon_i * c_i \quad (2)$$

where ϵ_i and c_i are the molar extinction coefficient and concentration of the i^{th} chromophore, respectively.

For pulse oximetry calculations, the change in light attenuation between peak systolic and diastolic time points (PPG pulse depth) is characterized at two wavelengths to derive the modulation ratio (R). Sometimes R is approximated using an amplitudinal measure of the pulse depth (AC) normalized to a non-pulsating (baseline) intensity (DC) and is valid for small changes in pulse amplitude [14].

$$R = \frac{\Delta A_{\lambda 1}}{\Delta A_{\lambda 2}} = \frac{\ln(I_{sys.,\lambda 1}/I_{dia.,\lambda 1})}{\ln(I_{sys.,\lambda 2}/I_{dia.,\lambda 2})} \approx \frac{(AC/DC)_{\lambda 1}}{(AC/DC)_{\lambda 2}} \quad (3)$$

In the conventional case, a single tissue is considered and it is assumed that the change in light intensity between systolic and diastolic events is mostly caused by pulsating arterial tissues that have similar path lengths. Since the hemoglobin derivatives in arterial blood primarily consist of HbO2 and Hb, it is also assumed that $SpO2 = c_{HbO_2}/(c_{Hb} + c_{HbO_2})$ and $(1 - SpO2) = c_{Hb}/(c_{Hb} + c_{HbO_2})$. Under these conditions, SpO2 can be derived in terms of the molar extinction coefficients (known) and R (measured):

$$SpO2 = \frac{\epsilon_{Hb,\lambda_1} - R * \epsilon_{Hb,\lambda_2}}{\epsilon_{Hb,\lambda_1} - \epsilon_{HbO_2,\lambda_1} + R * (\epsilon_{HbO_2,\lambda_2} - \epsilon_{Hb,\lambda_2})} \quad (4)$$

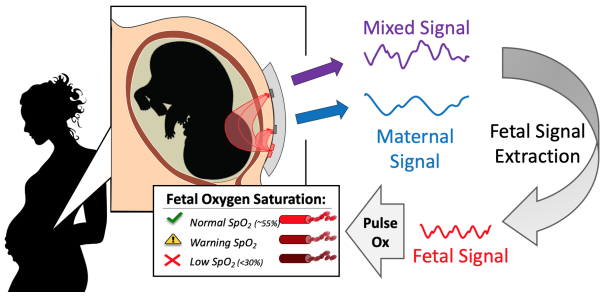

Fig. 1. High-level diagram of Transabdominal Fetal Pulse Oximetry [15].

For clinical pulse oximeters, the relationship between the modulation ratio and SpO2 is determined empirically through arterial blood gas analysis on a large number of subjects. Oftentimes, the wavelengths used to generate the modulation ratio exist on opposite sides of the isosbestic point of HbO2 and Hb (~805 nm), which maximizes the sensitivity to changes in hemoglobin concentration.

III. Transabdominal Fetal Pulse Oximetry

Transabdominal fetal pulse oximetry (TFO) is a fully non-invasive technique to measure fetal oxygen saturation. This is accomplished by sending photons into the tissue at the mother's abdomen to investigate the underlying fetal tissue. Since human tissue is a highly-scattering optical medium, many of these photons experience multiple scattering events before being extinguished through absorption, allowing them to propagate into deeper layers of tissue. Some of the photons that reach the fetus make it back to the skin-surface, where they can be captured by a photodetector as a light intensity signal and subsequently analyzed to estimate the fetal SpO2. Fundamentally, a light-based investigation is performed by sending a known light signal into the body, where it is modified by the tissue (e.g. absorbed or scattered) and measured some distance away. Considering the non-invasive nature of TFO, changes in both maternal and fetal tissue modify the propagating light, resulting in a *mixed* (maternal+fetal) signal. As such, the fetal portion of the mixed signal must be identified and extracted in order to calculate fetal SpO2. A high-level overview of this approach can be seen in Figure 1.

A. Characterizing the Mixed Signal

In TFO, changes in the maternal and fetal tissue composition are caused by various physiological systems. Thus, decomposing the mixed signal into its constituent components can be helpful. By expanding the dMBLL to consider the multiple tissues seen in TFO, we see that

$$\Delta A = \Delta\mu_{a,mat} * \langle L_{mat} \rangle + \Delta\mu_{a,fet} * \langle L_{fet} \rangle \quad (5)$$

where $\Delta\mu_{a,mat}$ and $\Delta\mu_{a,fet}$ are the changes in the absorption coefficients for maternal and fetal tissues accordingly, and $\langle L_{mat} \rangle$ and $\langle L_{fet} \rangle$ are the expected partial path-lengths photons take through the respective tissues before observation by a detector on the optode. To investigate the effects that maternal and fetal tissues have on the observed light intensity (i.e. mixed signal), we characterize relevant portions of the underlying physiological signals.

1) Cardiovascular Signals: Arterial vascular tissues expand slightly at each cardiac contraction, which results in a slight increase in the blood-tissue volume ratio and causes small modulations in the light intensity that occur periodically at the relevant heart rate (HR). Each modulation is characterized by a slight increase in the measured light intensity with diastolic relaxation, followed by a quick decrease during systolic contraction. The amplitudes of these signals are dependent on the vascular perfusion of the tissue being investigated, which typically range between 2-10%, and its blood content (e.g. hematocrit). In TFO, both maternal and fetal heart contractions affect the light intensity.

2) THM Waves: Artifacts seen in reflectance-based light intensity measurements are maternal Traube-Hering-Mayer (THM) waves. These are slow-moving (∼0.1 Hz) blood pressure waves that cause periodic modulations in the overall blood-tissue volume ratio. Independent of both respiratory and cardiac cycles, these normally-occurring waves are thought to be related to vasomotor contractions which are regulated by the autonomic nervous system [16].

3) Respiratory Signal: For abdominally-acquired measurements, the mother's respiratory system can significantly influence the acquired light intensity signal seen in TFO. These respiratory-induced intensity variations (RIIV) are seen in abdominally-acquired PPGs and are thought to be caused by the filling of the venous system and increased venous pressure [17]. Occurring synchronously with ventilation (inhalation and exhalation) at the respiratory rate (∼0.5 Hz), the intensity of these changes is dependent on parameters like tidal volume, body position, and probe location.

B. Extracting the Fetal Signal

To extract the fetal signal, superficial tissue regression, implemented through adaptive noise cancellation, can be used to filter out the maternal noise from the mixed signal, before performing frequency analysis to quantify the fetal signal parameters. This is accomplished by using near-far detector pairs to differentiate between the maternal and fetal information within the mixed signal. To elaborate on this approach, the measurements seen at a near and far detector are shown in Equations 6 and 7, respectively.

$$\Delta A_N = \Delta\mu_{a,mat} * \langle L_{mat}\rangle_N + \Delta\mu_{a,fet} * \langle L_{fet}\rangle_N \quad (6)$$

$$\Delta A_F = \Delta\mu_{a,mat} * \langle L_{mat}\rangle_F + \Delta\mu_{a,fet} * \langle L_{fet}\rangle_F \quad (7)$$

The depth of investigated tissue is proportional to the source-detector (SD) distance. Therefore, a near detector that is sufficiently close to the emitter will mostly capture photons that propagated through maternal tissue only ($\langle L_{fet}\rangle_N \approx 0$), whereas a far detector will capture both maternal+fetal information. As such, the difference in maternal-fetal information at the near-far detectors can be used to extract the fetal signal (ΔA_{fet}) by:

$$\Delta A_{fet} = \Delta\mu_{a,fet} * \langle L_{fet}\rangle_F = \Delta A_F - \alpha * \Delta A_N \quad (8)$$

where α is a ratio of the partial path-lengths through the maternal tissue seen at the two detectors, $\alpha = \langle L_{mat}\rangle_F / \langle L_{mat}\rangle_N$, which can be different for each patient and is generally unknown. Given this unknown factor, Equation 8 can be implemented in real-time through adaptive noise cancellation. Essentially, the near detector provides an estimate of the noise (from superficial tissues) that is corrupting the far detector's signal. Assuming that the signal and noise are uncorrelated, an adaptive algorithm can be used to remove the noise from the far signal. In other words, the noisy fetal signal (ΔA_F) can be improved by using an estimate of the maternal noise (ΔA_N) to adjust an adaptive filter (α) by minimizing the error in an optimization parameter (e.g. least-mean square).

To generate the modulation ratio (R), the signal is analyzed in the frequency domain, where the AC and DC parameters in Equation 3 are determined by identifying the respective magnitudes that correspond to the fundamental FHR frequency and 0 Hz. Note that the frequency domain analysis can also be done prior to adaptive noise cancellation. In particular, if the mixed signal contains a sufficient amount of fetal information, its power spectrum should contain a strong peak at the FHR (and its accompanying harmonics), corresponding to changes in the light intensity caused by the cardiac-induced arterial pulsations in fetal tissue. However, extracting the fetal signal through frequency analysis only (i.e., without removing maternal noise through adaptive noise cancellation) may fail if the fetal heart rate (∼110-160 bpm) overlaps with the maternal heart rate (∼60-100 bpm), which may occur more frequently during periods of fetal asphyxia. Reducing the maternal influence through adaptive noise cancellation prior to frequency analysis can help mitigate this effect.

C. Normal Levels of Adult vs Fetal Oxygen Saturation

Significant differences between the SpO2 levels of adults and fetuses can affect the evaluation of a pulse oximeter. Conventional pulse oximeters are evaluated on human adults in controlled desaturation experiments, which limits the accuracy of SpO2 values to a lower range of 70%. While this is acceptable for healthy adults, with typical SpO2 values between 90-100%, it is inappropriate for fetuses where normal SpO2 values are around 55%, with critical levels of fetal hypoxia at 30% or below [18]. Evaluating the TFO system on a set of *relevant* SpO2 values is an important step towards the development of a clinically-useful monitoring system. Note that differences in the absorption properties between adult and fetal hemoglobin are negligible for pulse oximetry [19], [20].

IV. TFO System Design and Development

To investigate this technique, we designed and developed a transabdominal fetal pulse oximetry (TFO) system to capture non-invasive measures of fetal SpO2. The TFO system (shown in Figure 2) consists of a multi-detector optode (optical probe), an embedded optode control system, and custom real-time software for visual feedback. In this section, we discuss the design aspects that were incorporated in each of the submodules to provide insight into the developed TFO system.

A. Multi-detector Optode

To perform TFO, the multi-detector optode is placed on the mother's abdomen just above the underlying fetus, where

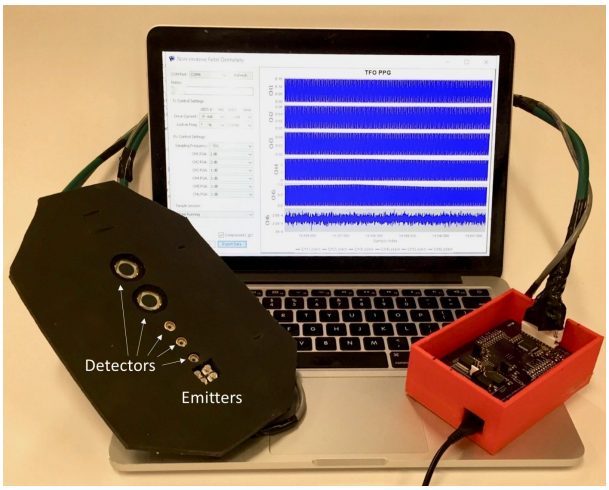

Fig. 2. A Transabdominal Fetal Pulse Oximetry (TFO) system was designed and developed. It consists of a multi-detector optode, embedded optode control system, and custom user-interface software.

photons are introduced into the body to investigate the tissue and are captured by a photodetector several centimeters away.

The high-scattering properties of human tissue cause photons to take a tortuous path through the tissue, causing significantly less light from reaching the underlying fetus. One approach to improve this is to send large amounts of photons into the body. Another approach is to optimize the wavelengths to reduce scattering and improve the depth of investigation. Typically, longer wavelengths scatter less, but have increased absorption properties in tissue. A balance between these two can be achieved by utilizing the near-infrared optical window. These wavelengths, between 650-950 nm, are often used to achieve penetration depths of up to several centimeters (optically deep) in oximetry-based systems [21]. To identify an optimal pair of wavelengths for TFO, Monte Carlo simulations were performed on a multi-layer tissue model, where the results showed that 740 nm and 850 nm wavelengths are optimal for capturing TFO signals [22]. As such, the TFO optode design utilizes these wavelengths to inject a large number of photons into the maternal abdomen using several high-power light emitting diodes (Marubeni), which are capable of emitting 560 mW and 1400 mW radiant power (740 and 850 nm, respectively). In regards to safety, the radiance levels used by the system are below thresholds set forth by IEC 60601-2-57, which classifies the system within the safest risk group. For clarity, we will refer to the 740 and 850 nm wavelengths as far-red and NIR, respectively.

In addition, the relative placement of a photodetector in relation to the emitter (source-detector or SD separation), greatly influences signal strength and investigated tissue depth. Using a small SD distance will result in a strong light intensity signal, but the photons it consists of would have only traversed superficial (maternal) tissues. Conversely, a large SD distance will capture photons that traversed through deeper (fetal) tissues, but the overall light intensity will be weaker, which might cause the fetal signal to fall below the noise floor of the detector. When designing an optode for TFO, careful consideration should be given to the SD distance to ensure that an appreciable fetal signal is captured. However, patient variability issues can cause a carefully designed optode to fail. One approach to solving this involves utilizing multiple detectors to improve spatial redundancy, but this runs the risk of over-complicating the hardware design. Striking a judicious balance can be accomplished by framing the issue as a multi-objective optimization problem, where hardware complexity and system performance on the population as a whole form competing objectives, to identify a Pareto-optimal optode design [15]. This approach was taken to guide the development of our multi-detector optode, which utilizes five, low-noise photodetectors (OSI Systems) with SD distances between 1.5 to 10 cm, enabling the detection of fetal depths of up to 5 cm. Note that the average fetal depth is 2.9 cm [23]. These photodetectors measure the diffuse reflectance and transform the radiant power from incident photons into an electrical current (photocurrent) through the inner photoelectric effect. By utilizing redundancy, the TFO system is more robust to both *inter-* and *intra-* patient variability by capturing information about multiple depths of tissue.

Importantly, the coupling between optical components and maternal tissue can influence the amount of light that is captured by a photodetector. Two common schemes to transfer photons are often used. One approach uses optical fibers to transport the photons to a remotely-housed photodetector, whereas the other simply moves the detector to be in close-contact with the tissue. Since the number of modes on an optical fiber often limits the transferrable light intensity, our multi-detector optode takes the latter approach which integrates the photodetectors into a flexible substrate. This is placed directly on the maternal abdomen to utilize the full active area and acceptance angle of the detectors.

To improve conformability and reduce ambient light levels, flexible black silicone (Rogers Corporation) was utilized as the substrate material for the optical components. Since the optode is in direct contact with the skin, silicone-based materials are suitable due to their non-irritant properties and are often used in medical products [24]. The size of the material was selected to block ambient light up to 6 cm away from the detector. This large coverage helped reduce the impact from the surgical lights that were in use during the animal study (Section V). In the clinical setting, the size can be reduced to be more appropriate for application on pregnant women. To reduce wiring constraints and allow the optode to conform to the skin, a thin copper-coated polyimide substrate was used as a flexible circuit board to interface the electronic circuitry with the optical components. The analog signal is transferred from the optical probe to the optode control system through a shielded-cable to reduce environmental noise effects.

B. Embedded Optode Control System

At the core of the TFO system is the embedded optode control system, which programmably controls the optical probe to inject a known light signal into the tissue and record the resulting diffuse reflectance observed by the photodetectors. Several key features of this submodule are the variable drive current to increase dynamic range on the emitter side, lock-in

detection to reduce flicker noise, programmable gain settings at each channel to improve the dynamic range and reduce quantization noise, and high-resolution digitization circuitry.

Increasing the drive current can improve the signal strength seen at a far detector. However, the recordable signal seen at closer detectors may saturate the acquisition circuitry. Capturing a signal at *both* near and far detectors may provide useful information to extract the fetal signal. Furthermore, natural differences in skin-tone between patients can increase the level of incident light needed to observe the fetal signal. Thus, to improve the dynamic range of the system, the optode control system allows the user to select an emitter drive current between 0 to 1000 mA. This allows a large number of photons to be generated, since only a small fraction of these are captured by a photodetector [22]. This was accomplished by using high-accuracy, programmable potentiometers with high-power current drivers (ON Semiconductors).

When a desired signal occurs at low frequencies, flicker (1/f) noise can have a significant effect on the signal ability to detect the signal. One approach to mitigate this is to utilize lock-in detection to modulate the desired signal at a higher frequency, which reduces the contamination from flicker noise. After detection, this higher-frequency signal can be demodulated (in either hardware or software) down to its baseband for conventional processing. In light-based systems, such as TFO, this can be accomplished by modulating the emitters at a higher frequency and synchronizing the activation signal with the detector measurements. Since the desired fetal signal occurs at these lower frequencies, the TFO system performs lock-in detection, accomplished by modulating the NIR and far-red light sources at 150 Hz and 330 Hz, respectively, and performing digital demodulation (software). These frequencies were sufficiently high to reduce flicker noise and were selected to avoid the influence from power lines (60 Hz + harmonics).

In TFO, the photocurrent that contains fetal information can be quite small (pico-amps). Thus, prior to digitization, the acquisition subsystem increases the strength of the small signal using several stages of amplification. The first gain stage uses transimpedance amplifiers to transform the small photocurrent signal into an amplified voltage signal which is more suitable for signal processing. Afterwards, the voltage signal goes through a secondary programmable-gain stage, which allows each of the incoming signals to be amplified 1, 2, 4, 8, or 12 times its original value. The programmability of the gain stages improves the adaptability of the TFO system to adjust to individual patients, as well as decreasing quantization noise. For completeness, these stages are implemented using two operational amplifiers in a differential configuration, where registers are used to programmably select appropriate gain values prior to the digitization circuitry.

After amplification, the resulting analog voltage signal is digitized through a high-resolution, $\Delta\Sigma$ analog-to-digital converter or ADC (Texas Instruments). The component performs simultaneous-sampling of all detector channels on the optode and provides 24 bits of resolution for each. This enables sampling at the sub-microvolt scale with a rate of up to 16 kHz, enabling digital demodulation. These measurements are then processed by a microcontroller, which uses an ARM Cortex M4 processor, to format and package the readings before streaming them to custom software running on a laptop for visual display, analysis, and recording. To integrate the various electronic components, we designed and assembled a printed circuit board, which sits inside of a unique 3D-printed housing to protect the components from the environment.

C. Custom Real-time Software

To allow a user to select appropriate measurement settings, we developed custom, user-interface (UI) software that provides a real-time graphical interface for controlling the TFO system settings, visualizing the incoming data, and recording the measurements for post-processing. Written in Java, the platform-agnostic software communicates with the embedded optode control system through a virtualized dual-COM port, which allows user-selectable measurement configurations and data to be sent to and from the embedded system simultaneously. The software converts the incoming, streaming data-packets into the raw ADC measurements from each detector. These are then transformed into associated voltage readings, and are presented in a real-time graph to provide visual feedback to the user. Simultaneously, the measurements are compressed and recorded in a datafile for further analysis and post-processing. Note that applying compression prior to writing large amounts of data to computer memory (hard disk) can improve processing efficiency. The UI software was designed using the well-established Model-View-Controller architecture, which improves the maintenance and reusability of the code through functionality-based modularization [25].

V. Experimental Methods

To evaluate the developed transabdominal fetal pulse oximetry system on a wide-range of fetal SpO2 values, we employed an *in utero* hypoxic fetal sheep model, where various levels of hypoxia were induced in a fetal lamb while recording both TFO measurements (non-invasive) and fetal arterial blood gases (invasive, gold standard).

A. Hypoxic Fetal Sheep Model

To employ a hypoxic fetal sheep model, the following procedures were performed. The procedures used were evaluated and approved by the UC Davis Institutional Animal Care and Use Committee and care for the animals adhered to the guidelines set forth by the Guide for the Care and Use of Laboratory Animals. After induction of anesthesia in an at term pregnant ewe (136 GA), a balloon catheter was inserted into the aorta and positioned above the uterine blood supply [26]. A laparotomy and hysterotomy were then performed to place an arterial blood line in the carotid artery of the fetus to allow for continuous hemodynamic monitoring and fetal blood sampling. To identify the location of the fetus throughout the experiments, a deterministic tissue geometry was created by suturing one ear of the fetal lamb to the underside of the ewe's abdominal wall, an approach used in other non-invasive measurement models [27], [28]. After replacing the lost amniotic fluid with warm saline, the rest

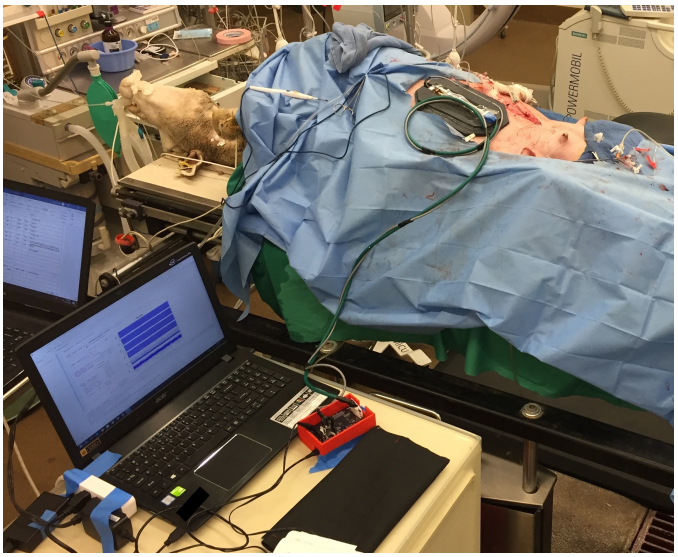

Fig. 3. A picture of the instrumental setup during the *in utero* hypoxic fetal lamb controlled desaturation experiments.

of the fetus was returned to the uterus and prior incisions were closed with suture. The right fetal forelimb remained exposed for the placement of a conventional pulse oximeter. An additional transmission-mode pulse oximeter was clipped onto the maternal ewe's abdominal wall at the laparotomy site to measure changes in oxygenation occurring in the more superficial (maternal) tissues. The TFO optode was placed on the maternal abdomen just above the underlying fetus, where the non-invasive light-based measurements were captured, and a black-out cloth was placed over the optode to reduce the effects of ambient light throughout the experiments. A picture of the experimental setup can be seen in Figure 3.

Varying degrees of fetal hypoxia were induced by reducing the blood flow to the uterine artery through partial-aortic occlusion (via inflation of the balloon catheter). This was performed in a graded fashion, where each level of hypoxia was held for 10 minutes while fetal arterial blood gases (ABGs) were recorded to derive the true fetal arterial oxygen saturation (SaO2). Arterial oxygen saturation derived from ABG analysis (ABL90 Flex, Radiometer Medical) is considered to be the gold standard. The maternal and fetal heart rates were recorded from conventional pulse oximeters and arterial blood pressure waveforms. The graded inflation continued until severe levels of fetal hypoxia were observed, evidenced by fetal SaO2 levels below 15%. At this point, the balloon was deflated and the fetus was allowed to recover. A total of three desaturation experiments were performed.

B. TFO System Parameters

In these experiments, the TFO system utilized drive currents of 600 mA to offer a large amount of light (320 mW for far-red and 840 mW for NIR sources) into the pregnant ewe's abdomen. The resulting diffused light intensity exiting the body was captured and converted into a voltage signal by the photodetectors and amplifiers with a gain of 10^6. The analog voltage readings were captured using the ADC, converted into data packets, and then streamed to the UI software for display and recording. Digital demodulation and frequency analysis were performed post-processing for convenience. Since lock-in detection was utilized to avoid 1/f contamination, a sufficiently high sampling rate (4 kHz) was selected to ensure that the modulated signals were fully captured to perform digital demodulation. For context, one hour of measurements at this sampling rate produces a data file with a size of about 500 MB. The data stream was compressed using the GZIP algorithm prior to being recorded in a datafile. Using synchronous detection, the signal from each wavelength was separated and corresponding power spectral densities were generated. Using Equation 3, these were used to identify the fetal contribution to the mixed signal and estimate fetal SpO2.

VI. Results

A snippet of the diffused, mixed light signal measured by the TFO system can be seen in Figure 4. Both the time-series measurements and corresponding power spectra are shown. Physiological changes in the tissue composition can be seen as strong peaks in the power spectrum, which occur at the corresponding fundamental frequencies (*solid arrows*) and their harmonics (*dotted arrows*). Decoupling maternal and fetal signals from the mixed-information light signal can be difficult to do in the time domain. Since the underlying physiological signal are periodic, analyzing the mixed signal in the frequency domain is more intuitive. By generating the power spectrum for each of these signals, the physiological components can be clearly seen. They are identified (and annotated) as the pregnant ewe's THM waves, respiratory rate (RR), and heart rate (MHR), as well as the fetal lamb's heart rate (FHR). The respiration and heart rates were confirmed through end-tidal CO2 monitoring and conventional pulse oximetry. To evaluate the long-term ability of TFO to identify these signals over time, spectrograms of the demodulated light intensity for each of the desaturation rounds are shown in Figure 5. As shown, the MHR ($\sim$2 Hz) and FHR ($\sim$2.4 Hz) can be clearly seen throughout each desaturation experiment, each lasting for about an hour.

As previously described, fetal hypoxia was induced at varying degrees while simultaneously measuring arterial oxygen saturation. For comparison reasons, the fetal oxygen saturation was derived using three different modalities, namely through arterial blood gases (SaO2 ABG, gold standard), a conventional pulse oximeter at the exposed fetal arm (SpO2 CPO), and through the developed TFO system (SpO2 TFO). The TFO- and CPO- derived fetal SpO2 values are shown against the true SaO2 ABG in Figure 6(a). A wide range of true fetal SaO2 ABG values were observed, ranging from a mean value of 62.7% at baseline (no inflation) to 13.5% at the most severe levels of hypoxia (most inflation). These changes were also captured by the non-invasive TFO system, which reported mean fetal SpO2 TFO values between 60.7% (baseline) to 15.2% (severe hypoxia). The root mean-squared error (RMSE) of the TFO measurements (compared to the gold standard) was 6.37%. For the detection of critical-levels of hypoxia (true SaO2 $<$ 30%), the RMSE value was 5.64% and the maximum absolute error was 10.4%.

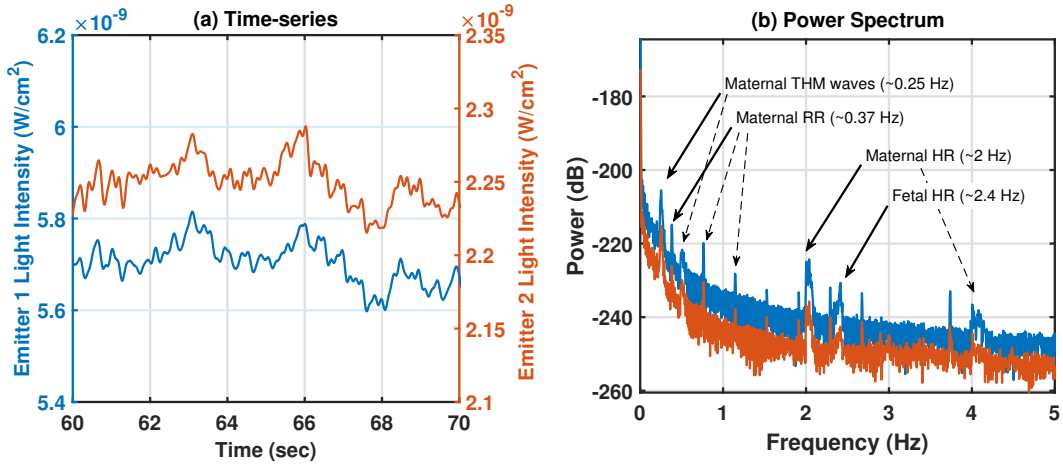

Fig. 4. An example of the mixed light intensity measurements (demodulated) captured by the TFO system, displayed in both **(a)** time and **(b)** frequency domain representations. Peaks in the power spectra correspond to physiological changes in the tissue (or their harmonics). Emitter 1 and 2 correspond to 850 nm and 740 nm wavelengths, respectively.

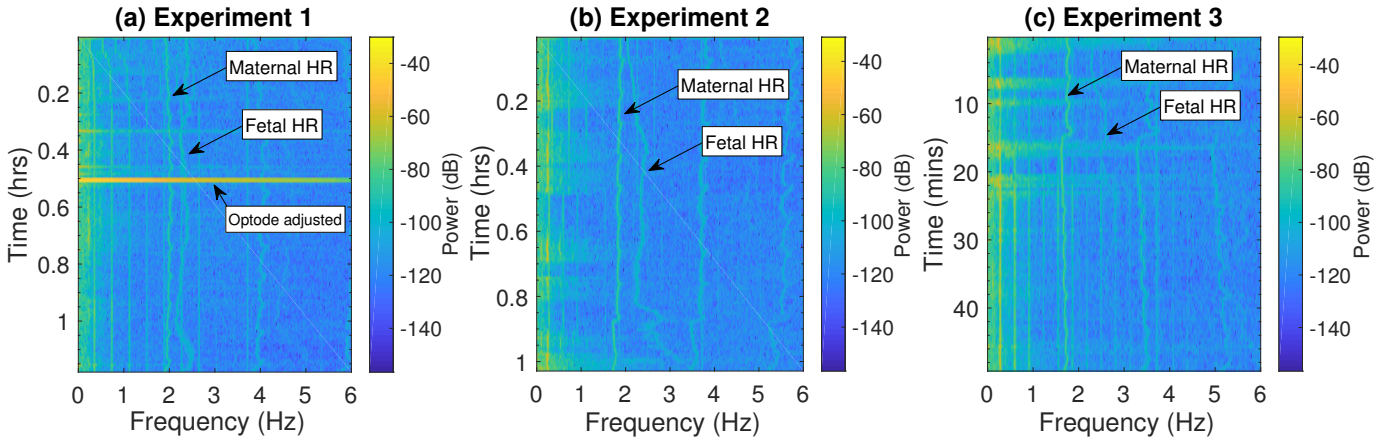

Fig. 5. Spectrograms of the intensity measurements (demodulated) captured during the desaturation experiments. The maternal and fetal HRs are annotated accordingly and can be seen for about one hour during each recording. The harmonics from the maternal HR can also be seen in each of the recordings. The optode was adjusted slightly in Experiment 1 to secure it to the abdomen of the pregnant ewe.

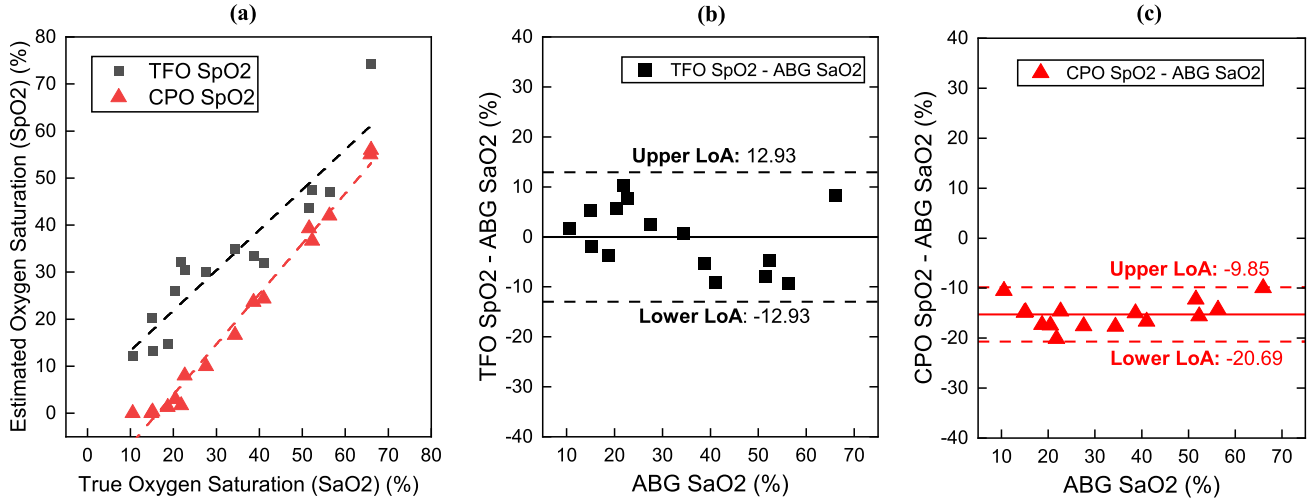

Fig. 6. Fetal arterial oxygen saturation measurements captured by gold standard arterial blood gases (ABG), conventional pulse oximeter at the exposed fetal arm (CPO), and the non-invasive transabdominal fetal pulse oximetry system (TFO). *(A)* Measurements from both TFO and CPO showed high correlation with the gold standard. *(B) and (C)* Bland-altman plots with the Limits of Agreement (LoA) shown for both TFO and CPO-derived SpO2 values.

For comparison, a conventional pulse oximeter (CPO) was placed on the exposed arm of the fetal lamb to capture another measure of fetal SpO2. The CPO-reported fetal SpO2 values ranged from 51.0% (baseline) to 0.11% (severe hypoxia), and had an RMSE value of 15.5%. For the detection of critical-levels of hypoxia, the RMSE was 16.2% and the maximum absolute error was 20.1%. The large error in CPO-reported fetal SpO2 values is expected and can be explained by the previously described inaccuracy of CPOs for low SpO2 levels [29]. Note that using CPO for the measurement of fetal SpO2 is similar to the transvaginal approach (discussed in Section VII) which is a *semi-invasive* method (invasive to mother, non-invasive to fetus), whereas TFO is a *fully non-invasive* method.

Several approaches were taken to evaluate the agreement between the non-invasive TFO, semi-invasive CPO, and invasive (gold standard) ABG methods. Quantitative measures of agreement were evaluated through correlation, significance tests, and Bland-Altman analyses [30]. As seen in Figure 6(a), both TFO and CPO measurements showed high correlation with the gold standard, evidenced by a Pearson's correlation-coefficient (r-value) of 0.925 for TFO and 0.991 for CPO, and a coefficient of determination (r-squared or r^2) of 0.856 for TFO and 0.984 for CPO. Using a paired student's t-test, it was determined that there were no significant differences between TFO-derived values and the gold standard at a significance level of $p>0.5$, suggesting strong agreement between the two methods. However, the same test identified significant differences between the CPO-reported measurements and the gold standard at a significance level of $p<0.05$, indicating poor agreement between CPO and the gold standard.

Further, Figure 6(b)-(c) show the Bland-Altman plots that were generated to compare TFO and CPO methods against the gold standard (ABG). Bland-Altman plots (also known as Tukey mean-difference plots) are commonly used to graphically present the differences between an experimental method with the gold standard. The Limits of Agreement (LoA) suggest the maximum error levels that should be tolerable if the new measurement method were to be used instead of the gold standard, and are defined as the mean difference $\pm$ 1.96 times the standard deviation of the differences. As shown, the worst-case LoA of the CPO-derived fetal SpO2 values is 20.7% below the true SaO2, whereas the TFO-derived values should be tolerable within 12.9% of the true SaO2. Note that in this case, the gold standard (ABG-derived fetal SaO2) is an invasive and clinically unavailable measure during pregnancy, whereas TFO presents an opportunity to observe this currently unresolved parameter.

One of the assumptions underlying the performance of TFO is that a sufficient amount of the observed light at the detector should have traversed fetal tissues. If this is not achieved, the mixed signal will reflect changes in the physiology occurring at the superficial (maternal) tissues only. To evaluate this in our experiments, the SpO2 of the pregnant ewe's abdominal tissue was monitored through a conventional pulse oximeter near the TFO optode. As shown in Figure 7, the ewe's abdominal SpO2 remained steady with a mean of 89%$\pm$7.4%, whereas

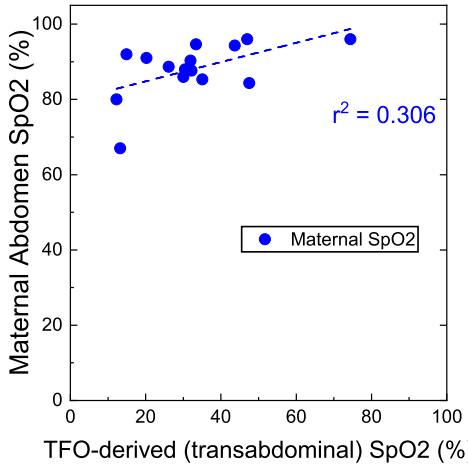

Fig. 7. Maternal ewe's abdominal vs TFO-derived (fetal) SpO2. The poor correlation suggests the TFO signal is expressing fetal physiology.

all TFO values remained below 74%. A paired student's t-test showed significant differences between the ewe's SpO2 and TFO-derived SpO2 values ($p<0.0001$). This improves our confidence that a sufficient amount of light penetrated the overlying maternal tissues and is reaching the underlying fetus.

VII. Discussion

This investigation highlights the non-invasive ability to measure fetal oxygen saturation through a novel transabdominal fetal pulse oximetry system on a hypoxic fetal lamb *in utero*. These types of measurements are currently unavailable in obstetric practice and has the potential to improve fetal outcomes by providing a more objective measure of fetal hypoxia. In addition, the transabdominal nature of the measurements enables future studies to evaluate the clinical utility of fetal SpO2 during the antepartum period of pregnancy. Previously, fetal SpO2 was only available during the intrapartum period through a transvaginal fetal pulse oximeter [31]. This semi-invasive method inserted an optode through the birth canal and onto the presenting fetal tissues, where conventional pulse oximetry was performed. This device was evaluated in a large randomized control trial, where it was shown that the addition of fetal SpO2 with CTG monitoring reduced the rates of C-sections due to NRFT [31]. The TFO system presented in this work provides a *fully non-invasive* alternative, which is placed on the mother's abdomen to conveniently measure fetal SpO2.

While this proof-of-concept study demonstrates the ability to measure fetal oxygen saturation on a relevant biological model, additional studies are needed to further characterize the operating limits of the technology. For example, the effects that labor dynamics can have on the TFO measurements are unknown, such as the effects of increases in uterine blood flow and interfacial pressure on the fetal tissues. In addition, to ensure that the TFO optode remained in an optimal location throughout the experiments, a deterministic tissue geometry was created by fixing the location of the fetal lamb relative to the maternal abdomen. However, spontaneous fetal movement, or improper placement of the optical probe above

the fetal tissue, can alter the ability of the system to accurately measure fetal SpO2. Additional models with varying anatomical characteristics can be useful in evaluating these effects. Furthermore, prospective studies involving pregnant women are needed to bridge the gap between pregnant sheep and pregnant humans towards eventual clinical use. However, this animal study provides an important step towards this goal by evaluating the TFO system on a wide-range of *known* fetal SaO2 values, which is otherwise unavailable prior to birth.

VIII. Related Work

Non-invasive fetal oximetry has been investigated by several groups in recent years. Some investigations evaluated light transport through representative tissue models of the *in utero* environment through simulation [32], [33]. Other studies evaluated fetal extraction approaches through signal processing techniques [34]–[37]. The creation of the mixed signal in most of these systems were primarily accomplished through simulations or emulated physical models. Other non-invasive approaches to measure fetal oxygen status were also considered [38]. Several studies involving pregnant mothers were able to use these systems to measure fetal SpO2 through sophisticated optical setups, yet studies involving their clinical utility have not been reported [39], [40].

IX. Conclusion and Future Work

In this paper, we presented a novel transabdominal fetal pulse oximetry system and discussed both design and development aspects. Furthermore, we evaluated its ability to non-invasively measure a wide range of fetal SpO2 on hypoxic fetal sheep *in utero*. The results highlight that the system has the potential to improve fetal outcomes by providing obstetricians with fetal SpO2 prior to birth in a non-invasive manner. We are currently investigating various aspects of the TFO system, including the effects of optode placement relative to the fetus, placental location, and active labor, and are continuing to improve the TFO system.

References

[1] B. Schifrin, "Fetal heart rate monitoring during labor," *JAMA*, vol. 222, no. 2, pp. 196–202, 1972.

[2] E. M. Graham *et al.*, "Intrapartum electronic fetal heart rate monitoring and the prevention of perinatal brain injury," *Obstetrics and Gynecology*, vol. 108, no. 3, pp. 656–666, Sep 2006.

[3] Z. Alfirevic *et al.*, "Continuous cardiotocography (ctg) as a form of electronic fetal monitoring (efm) for fetal assessment during labour," *Cochrane Database of Systematic Reviews*, no. 2, 2017.

[4] T. F. Nielsen and K.-H. Hökegård, "Cesarean section and intraoperative surgical complications," *Acta Obstetricia et Gynecologica Scandinavica*, vol. 63, no. 2, pp. 103–108, 1984.

[5] A. K. Hansen *et al.*, "Risk of respiratory morbidity in term infants delivered by elective caesarean section: cohort study," *BMJ*, 2008.

[6] J. A. Martin *et al.*, "Births: Final data for 2017," *National Vital Statistics Reports*, vol. 67, no. 8, pp. 1–50, 2018.

[7] E. L. Barber *et al.*, "Indications contributing to the increasing cesarean delivery rate," *Obstetrics and Gynecology*, vol. 118, no. 1, July 2011.

[8] World Health Organization, "Appropriate technology for birth," *The Lancet*, vol. 326, no. 8452, pp. 436 – 437, 1985.

[9] P. Nielsen *et al.*, "Intra- and inter- observer variability in the assessment of intrapartum cardiotocograms." *Acta Obstetricia et Gynecologica Scandinavica*, vol. 66, no. 5, pp. 421–4, 1987.

[10] K. B. Nelson *et al.*, "Uncertain value of electronic fetal monitoring in predicting cerebral palsy," *New England Journal of Medicine*, 1996.

[11] J. G. Webster, *Design of Pulse Oximeters (Book Series in Medical Physics and Biomedical Engineering)*, 1st ed. CRC Press, 1997.

[12] L. Kocsis *et al.*, "The modified beer–lambert law revisited," *Physics in Medicine and Biology*, vol. 51, no. 5, 2006.

[13] A. Sassaroli and S. Fantini, "Comment on the modified beer–lambert law for scattering media," *Physics in Medicine and Biology*, 2004.

[14] P. D. Mannheimer *et al.*, "Wavelength selection for low-saturation pulse oximetry," *IEEE TBME*, vol. 44, no. 3, pp. 148–158, March 1997.

[15] D. D. Fong *et al.*, "Optode design space exploration for clinically-robust non-invasive fetal oximetry," *ACM Transactions on Embedded Computing Systems*, vol. 18, no. 5s, 2019.

[16] C. Julien, "The enigma of mayer waves: Facts and models," *Cardiovascular Research*, vol. 70, no. 1, pp. 12–21, 2006.

[17] L. Nilsson *et al.*, "Macrocirculation is not the sole determinant of respiratory induced variations in the reflection mode photoplethysmographic signal," *Physiological Measurement*, vol. 24, no. 4, 2003.

[18] M. Kühnert *et al.*, "Predictive agreement between the fetal arterial oxygen saturation and fetal scalp ph: Results of the german multicenter study," *Am J of Obst. and Gyn.*, vol. 178, no. 2, pp. 330 – 335, 1998.

[19] A. Harris *et al.*, "Absorption characteristics of human fetal hemoglobin at wavelengths used in pulse oximetry." *J Clin Monit*, vol. 4, 1988.

[20] W. G. Zijlstra *et al.*, "Absorption spectra of human fetal and adult oxyhemoglobin, de-oxyhemoglobin, carboxyhemoglobin, and methemoglobin." *Clin Chem*, vol. 37, no. 9, pp. 1633–1638, Sep 1991.

[21] F. Scholkmann *et al.*, "A review on continuous wave functional near-infrared spectroscopy and imaging instrumentation and methodology," *NeuroImage*, vol. 85, no. Part 1, pp. 6 – 27, 2014.

[22] D. Fong *et al.*, "Transabdominal fetal pulse oximetry: The case of fetal signal optimization," in *2017 IEEE Healthcom*, Oct 2017.

[23] P. L. Carson *et al.*, "Fetal depth and ultrasound path lengths through overlying tissues," *Ultrasound in Medicine and Biology*, vol. 15, 1989.

[24] P. V. Mohanan and K. Rathinam, "Biocompatibility studies on silicone rubber," in *IEEE EMBS and Intl Conf of the BME Society of India*, 1995.

[25] B. Bates *et al.*, *Head First Design Patterns*. O'Reilly Media, 2009.

[26] K. Yamashiro *et al.*, "Fetal tolerance of maternal resuscitative endovascular balloon occlusion of the aorta in a sheep model," *American Journal of Obstetrics and Gynecology*, vol. 222, no. 1, pp. S718–S719, 2020.

[27] R. Choe *et al.*, "Transabdominal near infrared oximetry of hypoxic stress in fetal sheep brain in utero," *Proceedings of the National Academy of Sciences*, vol. 100, no. 22, pp. 12 950–12 954, 2003.

[28] D. D. Fong *et al.*, "Validation of a novel transabdominal fetal pulse oximeter in a hypoxic fetal sheep model," *Reproductive Sciences*, 2020.

[29] R. K. Webb *et al.*, "Potential errors in pulse oximetry," *Anaesthesia*, vol. 46, no. 3, pp. 207–212, 1991.

[30] R. Zaki *et al.*, "Statistical methods used to test for agreement of medical instruments measuring continuous variables in method comparison studies: A systematic review," *PLOS ONE*, vol. 7, no. 5, 2012.

[31] T. J. Garite *et al.*, "A multicenter controlled trial of fetal pulse oximetry in the intrapartum management of nonreassuring fetal heart rate patterns," *Am J of Obst and Gyn*, vol. 183, no. 5, pp. 1049–1058, 2000.

[32] A. Zourabian *et al.*, "Trans-abdominal monitoring of fetal arterial blood oxygenation using pulse oximetry," *Journal of Biomedical Optics*, vol. 5, no. 4, pp. 391–405, 2000.

[33] S. Ley *et al.*, *Simulation of Photon Propagation in Multi-layered Tissue for Non-invasive Fetal Pulse Oximetry*. Cham: Springer International Publishing, 2014, pp. 356–359.

[34] K. B. Gan *et al.*, *Adaptive Filtering Applications: Application of Adaptive Noise Cancellation in Transabdominal Fetal Heart Rate Detection Using Photoplethysmography*. InTech, June 2011, ch. 6.

[35] D. D. Fong *et al.*, "Recovering the fetal signal in transabdominal fetal pulse oximetry," *Smart Health*, vol. 9-10, pp. 23 – 36, 2018.

[36] M. Böttrich and P. husar, "Signal separation for transabdominal non-invasive fetal pulse oximetry using comb filters," in *2018 IEEE EMBC*, July 2018, pp. 5870–5873.

[37] D. D. Fong *et al.*, "Contextually-aware fetal sensing in transabdominal fetal pulse oximetry," in *Proceedings of the ACM/IEEE 11th International Conference on Cyber-Physical Systems*, 2020, pp. 119–28.

[38] N. Ramanujam *et al.*, "Antepartum, transabdominal near infrared spectroscopy: Feasibility of measuring photon migration through the fetal head in utero," *The Journal of Maternal-Fetal Medicine*, vol. 8, 1999.

[39] A. M. Vintzileos *et al.*, "Transabdominal fetal pulse oximetry with near-infrared spectroscopy," *American Journal of Obstetrics and Gynecology*, vol. 192, no. 1, pp. 129 – 133, 2005.

[40] N. Ramanujam *et al.*, "Photon migration through fetal head in utero using continuous wave, near infrared spectroscopy: clinical and experimental model studies," *Journal of Biomedical Optics*, vol. 5, no. 2, pp. 173–184, 2000.